Stem Cell Reports
Report
OPEN ACCESS

Krüppel-like Factor 4 Modulates Development of BMI1$^+$ Intestinal Stem Cell-Derived Lineage Following γ-Radiation-Induced Gut Injury in Mice

Jes G. Kuruvilla,[1,4] Chang-Kyung Kim,[1,4] Amr M. Ghaleb,[1] Agnieszka B. Bialkowska,[1] Calvin J. Kuo,[2] and Vincent W. Yang[1,3,*]
[1]Department of Medicine, Stony Brook University, Stony Brook, NY 11794, USA
[2]Department of Medicine, Stanford University School of Medicine, Stanford, CA 94305, USA
[3]Stony Brook University Medical Center, HSC T-16, Room 020, Stony Brook, NY 11794-8160, USA
[4]Co-first author
*Correspondence: vincent.yang@stonybrookmedicine.edu
http://dx.doi.org/10.1016/j.stemcr.2016.04.014

SUMMARY

In response to ionizing radiation-induced injury, the normally quiescent intestinal stem cells marked by BMI1 participate in the regenerative response. Previously, we established a protective role for Krüppel-like factor 4 (KLF4) in the intestinal epithelium where it reduces senescence, apoptosis, and crypt atrophy following γ-radiation-induced gut injury. We also described a pro-proliferative function for KLF4 during the regenerative phase post irradiation. In the current study, using a mouse model in which *Klf4* is deleted from quiescent BMI1$^+$ intestinal stem cells, we observed increased proliferation from the BMI1$^+$ lineage during homeostasis. In contrast, following irradiation, *Bmi1*-specific *Klf4* deletion leads to decreased expansion of the BMI1$^+$ lineage due to a combination of reduced proliferation and increased apoptosis. Our results support a critical role for KLF4 in modulating BMI1$^+$ intestinal stem cell fate in both homeostasis and the regenerative response to radiation injury.

INTRODUCTION

The mouse intestinal epithelium is renewed through intestinal stem cells (ISCs) every 3–4 days (Barker, 2014). The "stem cell zone" model identifying crypt base columnar (CBC) cells at the base of the intestinal crypt (Cheng and Leblond, 1974) and "+4 stem cell" model identifying a ring of cells above the CBC cells are two current models of ISCs (Buczacki et al., 2013). Leucine-rich G-protein-coupled receptor 5 (LGR5) marks active CBC stem cells (Barker et al., 2007), while B-cell-specific Moloney murine leukemia virus integration site 1 (BMI1) marks the +4 position quiescent ISCs (Sangiorgi and Capecchi, 2008). BMI1 is a component of the polycomb repressor complex, which functions in gene silencing (Luis et al., 2012). Other markers for the quiescent ISCs at the +4 position have also been identified (Montgomery et al., 2011; Powell et al., 2012; Takeda et al., 2011). Functional studies have demonstrated that BMI1$^+$ ISCs contribute to the regenerative response to ionizing radiation injury while LGR5$^+$ ISCs are susceptible and unable to lineage trace post-radiation injury (Yan et al., 2012).

Radiation injury to the gut is a common complication in patients undergoing cancer radiotherapy. Radiation causes extensive DNA damage followed by apoptosis, particularly in the actively proliferating cells of the gut, leading to gastrointestinal (GI) syndrome (Anno et al., 1989). Thus studying mechanisms by which the intestinal epithelial cells regenerate in response to radiation is important for developing strategies to minimize injury resulting from ionizing irradiation. The zinc-finger transcription factor Krüppel-like factor 4 (KLF4) is expressed in the intestinal epithelium, promotes cellular differentiation, and contributes to epithelial homeostasis (Ghaleb et al., 2011). KLF4 also exhibits an anti-apoptotic activity to γ-irradiation in vitro by inhibiting the p53-mediated apoptosis (Ghaleb et al., 2007a). In vivo, we demonstrated that deletion of *Klf4* from the intestinal epithelium has a detrimental effect on the survival of mice following total body irradiation (Talmasov et al., 2014). In the short term, after irradiation KLF4 suppresses both apoptosis and proliferation and assists in DNA damage repair (Talmasov et al., 2014). In contrast, during the regenerative phase following irradiation, KLF4 plays an opposite role by promoting crypt cell survival and proliferation (Talmasov et al., 2014). KLF4 therefore exerts a context-dependent activity in the gut epithelium in response to ionizing irradiation. This context-dependent nature of KLF4's transcriptional activity has previously been observed in vitro (Rowland and Peeper, 2006).

To reconcile the dichotomy between KLF4's cytostatic nature at homeostasis and pro-proliferative activity during regeneration subsequent to irradiation, we determined the contribution of KLF4 in controlling the fate of BMI1$^+$ ISCs by lineage tracing. Our results indicate that KLF4 is a critical factor that determines the proliferative potential of BMI1$^+$ stem cell-derived lineage.

RESULTS AND DISCUSSION

KLF4 Is Expressed in Isolated Intestinal Crypt Epithelial Cells

KLF4 is expressed along the entire length of the mouse intestine (Ghaleb et al., 2005), mainly in the non-proliferating, terminally differentiated epithelial cells (Shields et al., 1996; Ghaleb et al., 2007b). Immunofluorescence (IF) staining of the mouse intestine for KLF4 shows the presence of isolated KLF4$^+$ cells in the crypts (Figures 1Ab and 1Ag) in addition to an increasing gradient of expression toward the lumen in cells lining the villus border (Figure 1Ab). To determine the proliferative state of the isolated KLF4$^+$ crypt cells, we co-stained the tissue for KLF4 and the proliferation marker, MKI67 (Gerdes et al., 1983). As shown in the example in Figure 1Ai, the majority of KLF4$^+$ cells in the crypts do not co-stain with MKI67. A close examination of the crypts showed that many of the KLF4$^+$/MKI67$^-$ cells are located in the +4 position of the stem cell zone (Figures 1Ag and 1Ai; arrows). These results are consistent with previous findings that illustrate the anti-proliferative activity of KLF4 (Ghaleb et al., 2005; McConnell et al., 2007).

KLF4 Is Expressed in a Subpopulation of BMI1$^+$ Cells in the Intestinal Crypts

The quiescent stem cell at the +4 position has been shown to express BMI1 (Sangiorgi and Capecchi, 2009) and is considered the "reserve" stem cell (Barker, 2014). Given that the crypt KLF4$^+$ cells are quiescent, we asked whether the BMI1$^+$ quiescent stem cells also express KLF4. We examined the intestine of *Bmi1*-Cre^{ER};Rosa26^{eYFP} mice, in which tamoxifen induction of Cre activity in BMI1$^+$ cells results in enhanced yellow fluorescent protein (eYFP)-guided lineage tracing (Sangiorgi and Capecchi, 2008). The tissue was co-stained for KLF4 to determine the extent to which crypt cells co-express KLF4 and eYFP. Two days following tamoxifen administration, eYFP$^+$ cells are present in a distinct number of epithelial cells in the crypts (Figures 1Bb and 1Bg). As in Figure 1Ag, KLF4 is expressed in cells around the +4 position in the crypt (Figure 1Bh). Importantly a subpopulation of eYFP$^+$ cells (average 19.0% ± 3.3%) also co-stained for KLF4 in the crypt epithelium (Figures 1Bi and 1Bj, arrow).

We then determined the proliferative status of eYFP$^+$ cells with or without KLF4 by triple immunostaining against eYFP, KLF4, and 5-ethynyl-2′-deoxyuridine (EdU) (see Figure 2A for an example). As shown in Figure 2B, four subpopulations of eYFP$^+$ cells are found in the crypts: (1) KLF4$^+$/EdU$^-$ (16.4%; red); (2) KLF4$^+$/EdU$^+$ (2.6%; orange); (3) KLF4$^-$/EdU$^+$ (37.2%; magenta); and (4) KLF4$^-$/EdU$^-$ (43.8%; green). It is clear that the majority of eYFP$^+$/KLF4$^+$ cells are EdU$^-$, indicating that they are quiescent. Importantly more than 86% of the eYFP$^+$/KLF4$^+$/EdU$^-$ cells are located at +4 position of the crypt (Figure 2B). These results indicate that KLF4 marks a unique population of quiescent BMI1$^+$ cells at the +4 position of the intestinal crypt. Among the eYFP$^+$/KLF4$^-$ cells, approximately half are EdU$^+$ and the other half EdU$^-$. They presumably represent descendants of the BMI1 lineage either in the process of dividing (EdU$^+$) or fully differentiated (EdU$^-$).

Previous studies indicate that while BMI1$^+$ ISCs minimally contribute to homeostatic renewal, they are critical in repopulating the intestinal epithelium following γ-irradiation (Yan et al., 2012). Given that KLF4 is expressed in a subpopulation of BMI1$^+$ crypt cells at the +4 position (Figure 2) and that KLF4 contributes to the regenerative process following irradiation (Talmasov et al., 2014), we investigated the role of KLF4 in modulating proliferation and lineage determination of BMI1$^+$ cells in vivo. We crossed *Bmi1*-Cre^{ER};Rosa26^{eYFP} mice (Ctrl) with *Klf4*$^{fl/fl}$ mice (Ghaleb et al., 2011) to generate *Bmi1*-Cre^{ER};Rosa26^{eYFP};*Klf4*$^{fl/fl}$ mice (denoted *Bmi1*$^{\Delta Klf4}$) to examine the effect of *Klf4* deletion from BMI1$^+$ cells during homeostasis and after radiation. The experimental schema is illustrated in Figure S1.

Klf4 Deletion from BMI1$^+$ Cells in Non-irradiated Mice Leads to Increased Lineage Tracing

Figure 3 shows the effect of *Klf4* deletion from *Bmi1*-expressing cells at homeostasis. In non-irradiated control (Ctrl-Sham) mice, eYFP$^+$ cells were detected on days 2 and 6 after tamoxifen treatment (Figures 3Aa and 3Ab) with day 6 trending higher than day 2, but did not reach statistical significance (Figure 3B). In contrast, the number of eYFP$^+$ cells was significantly increased in the crypts of *Bmi1*$^{\Delta Klf4}$-sham mice on day 6 compared with day 2 after tamoxifen treatment (Figure 3B; $p < 0.01$). Moreover, the number of eYFP$^+$ cells in the crypts of *Bmi1*$^{\Delta Klf4}$-sham mice was significantly higher than that of Ctrl-Sham mice on day 6 after tamoxifen treatment (Figure 3B; $p < 0.05$). In *Bmi1*$^{\Delta Klf4}$-sham mice, there was a near complete absence of KLF4-expressing cells in the crypts that contain BMI1$^+$ lineages 6 days after tamoxifen treatment (Figure 3Ap). These results indicate that lineage tracing from BMI1$^+$ crypt cells is increased when *Klf4* is deleted from them, suggesting that one of KLF4's functions during homeostasis is to maintain the quiescent state of BMI1$^+$ ISCs. This is consistent with studies that support an anti-proliferative function of KLF4 in the intestinal epithelium (Ghaleb et al., 2011; Shields et al., 1996).

We also examined the proliferative states of eYFP$^+$ crypt cells after tamoxifen administration in control and *Bmi1*$^{\Delta Klf4}$ mice. In control mice the number of

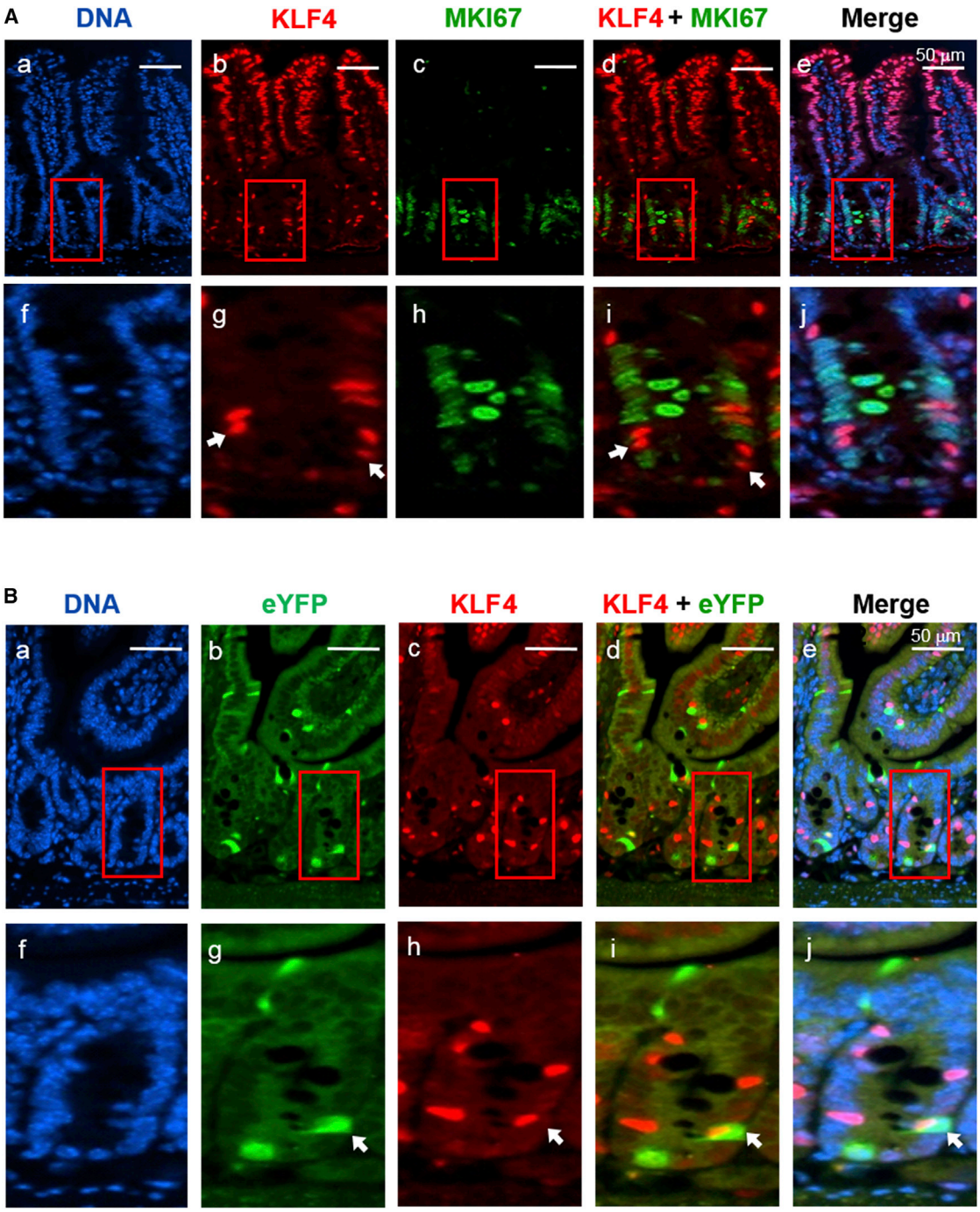

Figure 1. KLF4 Is Expressed in a Subpopulation of Crypt Epithelial Cells that Express BMI1

(A) Immunostaining of an adult mouse intestine showing DNA (a, f), KLF4 (b, g), and MKI67 (c, h). Panels (f)–(j) are magnified views of the boxed areas in panels a–e, respectively. Arrows mark KLF4-positive cells at +4 position that do not co-stain with MKI67. Panels (d) and (i) are merged images of KLF4 and MKI67 stains, while (e) and (j) are merged images of all three stains.

(B) KLF4 is expressed in a subpopulation of BMI1^{+} cells. *Bmi1*-Cre^{ER};Rosa26^{eYFP} mice were injected with tamoxifen to induce recombination. Intestines were collected 2 days after injection and analyzed by IF staining for DNA (a, f), eYFP (b, g), and KLF4 (c, h). Panel (d) is the merge of KLF4 and eYFP stains and (e) is a merge of all three. Panels (f)–(j) are magnified views of the boxed areas in (a)–(e), respectively. The arrows indicate a KLF4 and eYFP co-positive cell in the crypt.

Scale bars, 50 μm.

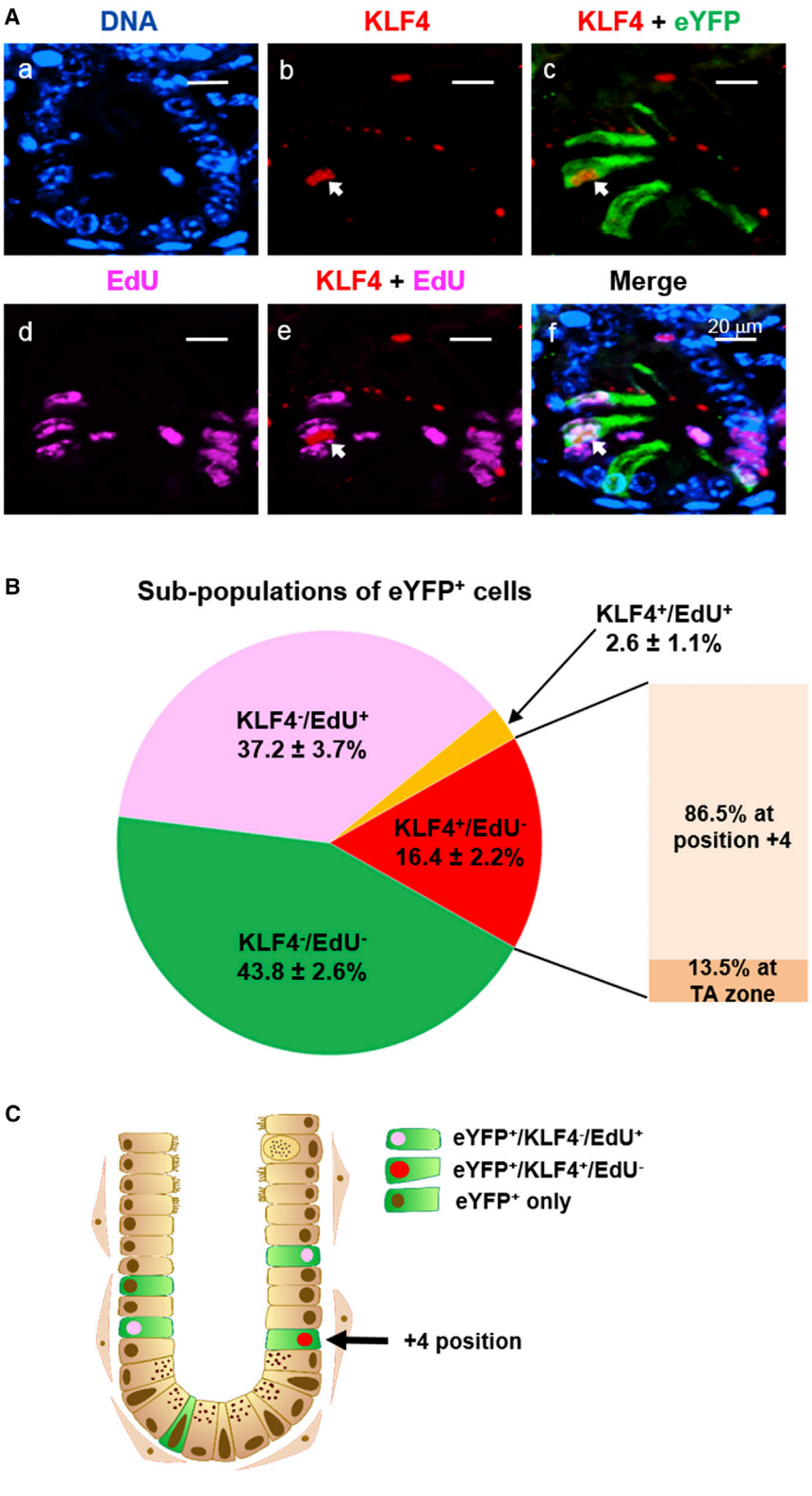

Figure 2. Differential Expression of KLF4 in BMI1$^+$ Cells and Their Proliferation Profile

(A) Intestines from *Bmi1*-Cre^{ER};Rosa26^{eYFP} mice were collected 2 days after tamoxifen injection. Mice were injected with EdU 4 hr prior to euthanasia. IF staining was performed for eYFP (green), KLF4 (red) and EdU (magenta). Panel (c) is a merged image of KLF4 and eYFP; (e), KLF4 and EdU; and (f), all three. The arrows point to an eYFP$^+$/KLF4$^+$/EdU$^-$ cell. Scale bars, 20 μm.

(B) Distribution of BMI1$^+$ cells in the crypts according to the status of KLF4 and EdU. A total of 50 crypts containing eYFP$^+$ cells were counted per mouse (n = 3). The pie chart shows the subpopulations of eYFP$^+$ cells distinguished by co-staining with KLF4 and/or EdU. The column displays the percentage of eYFP$^+$/KLF4$^+$/EdU$^-$ cells that are at the +4 position or within transit amplifying (TA) zone.

(C) A schematic representation of differential BMI1$^+$ lineage tracing in the intestines of *Bmi1*-Cre^{ER};Rosa26^{eYFP} mice 2 days after tamoxifen injection. The illustration shows the locations of various subpopulations of BMI1$^+$ cells in the crypt. Cells that are eYFP$^+$ alone are observed at different positions in the crypt. eYFP$^+$/KLF4$^+$/EdU$^-$ cells are predominantly observed in the +4 region.

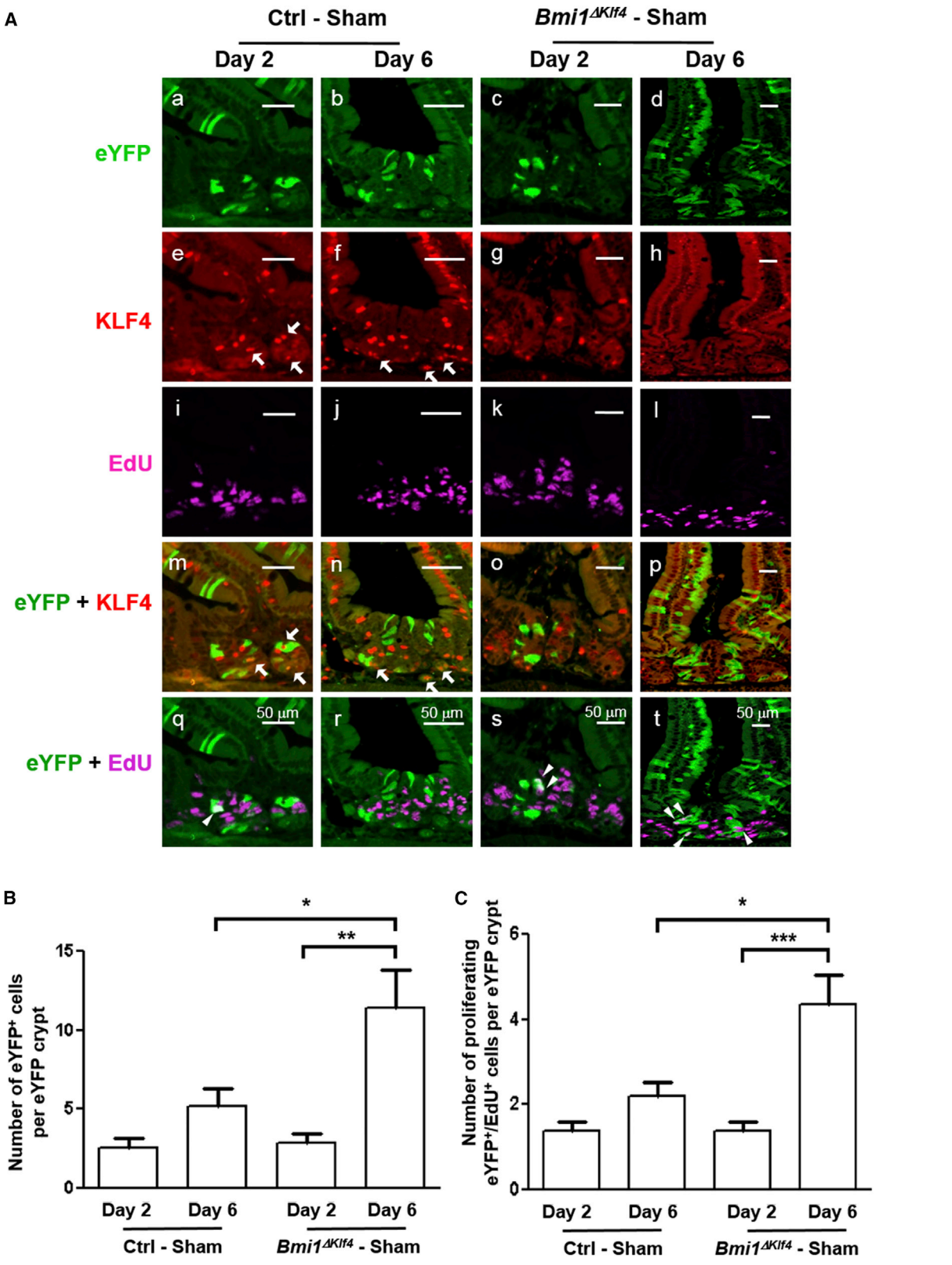

(legend on next page)

eYFP$^+$/EdU$^+$ cells accounted for a minority of eYFP$^+$ cells in the crypt on day 2 and remained so on day 6 (Figures 3Aq and 3Ar). In contrast, the number of eYFP$^+$/EdU$^+$ crypt cells increased significantly from days 2 to 6 in *Bmi1*$^{\Delta Klf4}$ mice (Figures 3As, 3At, and 3C; $p < 0.001$). Moreover, the number of eYFP$^+$/EdU$^+$ crypt cells in *Bmi1*$^{\Delta Klf4}$ mice was significantly higher than that in control mice on day 6 after tamoxifen treatment (Figure 3C; $p < 0.05$). These results lend support to the anti-proliferative function of KLF4 in maintaining quiescence of a subpopulation of BMI1$^+$ stem cells during homeostasis. In the absence of KLF4, BMI1$^+$ cells are able to re-enter the cell cycle faster and initiate lineage tracing more effectively.

KLF4 Facilitates Expansion of BMI1$^+$ Cell-Derived Lineage Following Irradiation

Previous studies demonstrate that BMI1$^+$ ISCs are radioresistant and contribute to clonal expansion of epithelial cells during the regenerative phase following γ-irradiation (Yan et al., 2012). We recently showed that mice with intestine-specific deletion of *Klf4* are more susceptible to radiation-induced gut injury than mice with intact *Klf4* (Talmasov et al., 2014). This is due to the ability of KLF4 to inhibit apoptosis during the acute phase of radiation injury and to contribute to crypt regeneration during the regenerative phase following irradiation (Talmasov et al., 2014). Here we sought to determine whether KLF4 is involved in the clonal expansion of BMI1$^+$ cell lineage after radiation. Using the schema depicted in Figure S1, we performed lineage tracing of eYFP$^+$ cells in irradiated control (Ctrl-Irr) and irradiated *Bmi1*$^{\Delta Klf4}$ (*Bmi1*$^{\Delta Klf4}$-Irr) mice that received 12 Gy total body γ-irradiation 2 days after the administration of tamoxifen. Clones of eYFP$^+$ cells were detected in the intestine of both Ctrl-Irr and *Bmi1*$^{\Delta Klf4}$-Irr mice 96 hr following irradiation (6 days after tamoxifen administration) (see Figure 4A for an example; additional examples are provided in Figure S2). Consistent with previous findings (Talmasov et al., 2014), abundant KLF4$^+$/EdU$^+$ cells were present in the regenerating crypts of Ctrl-Irr mice and this was irrespective of the status of eYFP expression (Figures 4Aa–4Ae). In contrast, there were fewer KLF4$^+$/EdU$^+$ cells in the eYFP$^+$ clones compared with neighboring eYFP$^-$ crypts in *Bmi1*$^{\Delta Klf4}$-Irr mice (Figures 4Ag–4Aj). Quantitatively the numbers of both eYFP$^+$/EdU$^+$ and total eYFP$^+$ cells were significantly smaller in eYFP$^+$ crypts of *Bmi1*$^{\Delta Klf4}$-Irr mice compared with Ctrl-Irr mice (Figures 4C and 4D, respectively; $p < 0.001$). These differences correlated with a significant reduction in the number of eYFP$^+$/KLF4$^+$ cells in the crypts of *Bmi1*$^{\Delta Klf4}$-Irr mice compared with Ctrl-Irr mice (Figure 4B; $p < 0.001$). Furthermore, the average total surface area (in μm^2) of eYFP$^+$ clones in *Bmi1*$^{\Delta Klf4}$-Irr mice was significantly smaller than that of Ctrl-Irr mice (Figure 4E; $p < 0.001$). Taken together, these results demonstrate that reduction of KLF4 from BMI1$^+$ cells restricts their clonal expansion after irradiation.

We previously demonstrated KLF4 as an anti-apoptotic factor that promotes survival post irradiation (Talmasov et al., 2014). Apoptotic cell death in eYFP$^+$ crypts of both sham and irradiated Ctrl and *Bmi1*$^{\Delta Klf4}$ mice was analyzed on day 6 after tamoxifen treatment using the TUNEL staining assay. A negligible number of apoptotic epithelial cells was observed in eYFP$^+$ clones of sham control and *Bmi1*$^{\Delta Klf4}$ mice (Figures S3Aa, S3Ab, S3Ae, S3Af, and S3B). Following irradiation there was an increase in the number of apoptotic cells compared with sham-irradiated mice in the respective genotype (Figure S3B; $p < 0.001$). Importantly the number of apoptotic cells in eYFP$^+$ clones was considerably higher in the *Bmi1*$^{\Delta Klf4}$-Irr group compared with the Ctrl-Irr group (Figures S3Ac, S3Ad, S3Ag, S3Ah, and S3B; $p < 0.0001$). Taken together, the results indicate that the ability of KLF4 to facilitate clonal expansion of the BMI1$^+$ lineage during the regenerative phase after irradiation is due to a combination of its anti-apoptotic and pro-proliferative effects.

The results of the current study delineate several subpopulations of eYFP$^+$ cells in the intestinal crypts 2 days after Cre-recombinase induction. Although the percentage of eYFP$^+$ cells that co-expresses KLF4 is relatively small (19%), it is notable that the majority of eYFP$^+$/KLF4$^+$ cells are EdU$^-$ and the majority of them reside in the +4

Figure 3. Deletion of *Klf4* in BMI1$^+$ Cells during Homeostasis Leads to Increased BMI1$^+$ Lineage Tracing

(A) Control (Ctrl) and *Bmi1*$^{\Delta Klf4}$ mice in the sham group were injected with tamoxifen and intestines were collected on days 2 and 6. IF staining was performed for eYFP that traces cells of the BMI1$^+$ lineage (a–d; green), KLF4 (e–h; red), and EdU (i–l; magenta). Panels (m)–(p) are merged images of eYFP and KLF4, and panels (q)–(t) are merged images of eYFP and EdU. Arrows indicate eYFP and KLF4 co-positive cells and arrowheads indicate eYFP and EdU co-positive cells. Scale bar calibrations for each column are shown on the bottom row.

(B) Quantification of the number of eYFP$^+$ cells per crypt in the intestines of Ctrl and *Bmi1*$^{\Delta Klf4}$ mice on days 2 and 6 after tamoxifen treatment. A total of 50 crypts containing eYFP$^+$ cells were counted per mouse (n = 3 per group).

(C) Quantification of the number of eYFP$^+$/EdU$^+$ cells per eYFP crypt of Ctrl and *Bmi1*$^{\Delta Klf4}$ mice on days 2 and 6 after tamoxifen administration. A total of 50 crypts containing eYFP$^+$ cells were counted per mouse (n = 3 per group).

For (B) and (C), statistical analysis was performed using a linear mixed model for repeated measurements with SAS 9.3 (SAS Institute). *$p < 0.05$; **$p < 0.01$; ***$p < 0.001$. Bars represent the SEM.

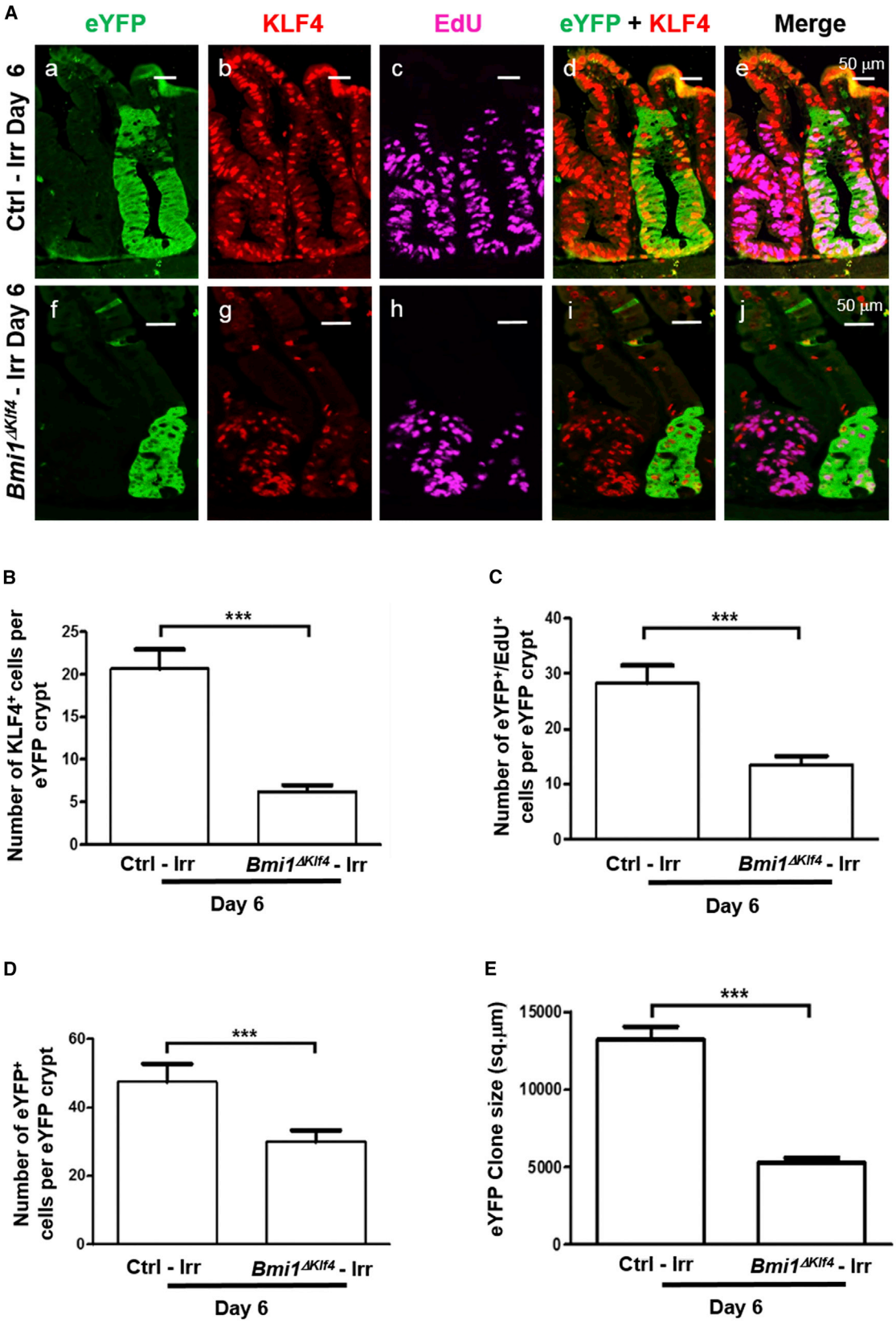

(legend on next page)

position of the intestinal crypts (Figure 2B). This observation suggests that KLF4 marks a unique population of BMI1-expressing crypt cells that are quiescent at homeostasis. As ionizing radiation preferentially targets actively cycling cells, the $BMI1^+/KLF4^+$ cells would be radioresistant while dividing cells ($eYFP^+/EdU^+$) (many of which are located in the transit amplifying zone) are radiosensitive. Given that the normally quiescent $BMI1^+$ cells rapidly proliferate to repopulate the intestinal crypts after irradiation (Yan et al., 2012) and that the regenerated crypts contain a relatively high number of $KLF4^+$ cells that are proliferating (Talmasov et al., 2014 and this study), it is likely that the +4 position BMI1 cells which express KLF4 are a source of clonal expansion during the regenerative phase after irradiation.

The differential effect of KLF4 in modulating proliferative capacity of $BMI1^+$ ISCs at homeostasis and during post-irradiation regeneration is intriguing. Our results demonstrate that the homeostatic function of KLF4 is to maintain $BMI1^+$ cells in a quiescent state, whereas KLF4 exerts a pro-proliferative activity on $BMI1^+$ cell-derived lineage after irradiation. The exact mechanism by which KLF4 promotes cell proliferation in the intestinal epithelium following radiation injury is not clear, although previous studies have demonstrated that KLF4 can exert its activities in a context-dependent manner (Rowland et al., 2005). In cancer it is also known that KLF4 can either be a tumor suppressor or an oncoprotein, depending on the tissues of origin (Evans and Liu, 2008; McConnell et al., 2007). Here we show that reduced clonogenic capacity of BMI1 cell-derived lineage in the absence of KLF4 after irradiation is the combined result of reduced proliferation (Figure 4) and increased apoptosis (Figure S3). The anti-apoptotic activity of KLF4 following γ-radiation-induced DNA damage has previously been observed in vitro and is thought to be mediated by the ability of KLF4 to inhibit transactivation of the proapoptotic BAX gene by p53 (Ghaleb et al., 2007a). The exact mechanism by which KLF4 switches roles from an anti-proliferative to a pro-proliferative factor during the regenerative phase after irradiation is less clear. Given that expression of KLF4 in the intestinal epithelium is regulated by the Wnt and Notch pathways (Ghaleb et al., 2008; Zhang et al., 2006), it is plausible that either the Wnt, Notch, or both pathways are perturbed following ionizing radiation (Davies et al., 2008), converting the normally cytostatic function of KLF4 to a pro-proliferative one.

A recent study further highlights the significance of reserve ISCs in mediating epithelial regeneration following tissue damage. Roche et al. (2015) demonstrated that a subset of crypt-based cells with high levels of SOX9, shown also to be the label-retaining cells (LRCs), co-express markers of active (e.g. LGR5) and reserve ISCs (including BMI1). In these cells, SOX9 limits the proliferation of LRCs at basal state but imparts radiation resistance. Thus, mice with intestine-specific deletion of *Sox9* lost their regenerative capacity following radiation damage (Roche et al., 2015). These results are reminiscent of the role of KLF4 in mediating epithelial regeneration after radiation injury described here and previously (Talmasov et al., 2014). It is also of interest to know that both KLF4 and SOX9 were shown to antagonize Wnt signaling in cancer cells by inhibiting β-catenin and TCF activity (Sellak et al., 2012). Whether KLF4 and SOX9 function synergistically to regulate reserve ISC function under basal conditions and/or following radiation injury requires further investigation.

In summary, the results of our study demonstrate that KLF4 modulates the fate of $BMI1^+$ ISCs in vivo and contributes to crypt regeneration from the $BMI1^+$ cell-derived lineage by promoting its clonal expansion after γ-irradiation. These results support a role for KLF4 in modulating plasticity of ISCs and protecting the intestine from radiation-induced injury.

EXPERIMENTAL PROCEDURES

Mouse Strains and Treatments

Bmi1-Cre^{ER} mice (The Jackson Laboratory) were crossed with B6-$Rosa26^{eYFP}$ to obtain *Bmi1*-Cre^{ER};$Rosa26^{eYFP}$ mice, designated as Ctrl. The *Klf4* deletion mutant was generated by breeding the control mice with $Klf4^{fl/fl}$ previously described in Ghaleb et al. (2011) to generate *Bmi1*-Cre^{ER};$Rosa26^{eYFP}$;$Klf4^{fl/fl}$, designated as $Bmi1^{\Delta Klf4}$. Protocols for tamoxifen administration and

Figure 4. Deletion of *Klf4* in $BMI1^+$ Cells Leads to Decreased Expansion of the $BMI1^+$ Lineage after γ-Irradiation

(A) Ctrl and $Bmi1^{\Delta Klf4}$ mice were injected with tamoxifen and subjected to 12 Gy total body irradiation on day 2 after injection. Tissues were collected on day 6 after injection (day 4 after irradiation). IF staining of eYFP (green), KLF4 (red), and EdU (magenta) in the intestine of Ctrl and $Bmi1^{\Delta Klf4}$ mice was performed and a representative result is shown. Scale bars, 50 μm.

(B) Quantification of $KLF4^+$ cells in $eYFP^+$ crypts in irradiated Ctrl and $Bmi1^{\Delta Klf4}$ mice at day 6 after tamoxifen administration.

(C) Quantification of EdU^+ cells in $eYFP^+$ crypts in irradiated Ctrl and $Bmi1^{\Delta Klf4}$ mice at day 6 after tamoxifen administration.

(D) Quantification of $eYFP^+$ cells in the $BMI1^+$ lineage in irradiated Ctrl and $Bmi1^{\Delta Klf4}$ mice at day 6 after tamoxifen administration.

(E) Quantification of the total surface area in μm^2 occupied by the $BMI1^+$ lineage ($eYFP^+$ crypts) in irradiated Ctrl and $Bmi1^{\Delta Klf4}$ mice on day 6. A total of 16 $eYFP^+$ crypts were measured per mouse (n = 4 per group). Data represent averages ± SEM. ***$p < 0.001$.

For (B), (C), and (D), a total of 16 crypts were counted per mouse (n = 4 per group). Data represent averages ± SEM. ***$p < 0.001$.

γ-irradiation procedures are described in Supplemental Experimental Procedures. All animal studies were approved by the Stony Brook University Institutional Animal Care and Use Committee (IACUC).

Tissue Preparation

Small intestines harvested from euthanized mice were flushed with modified Bouin's fixative (50% ethanol, 5% acetic acid) and cut open longitudinally. The intestines were Swiss-rolled, fixed, and embedded in paraffin. Five-micrometer-thick sections were cut for IF staining at the Department of Pathology of Stony Brook University.

Immunofluorescence

For immunostaining, sections were de-paraffinized in xylene, incubated in 3% hydrogen peroxide in methanol for 30 min, rehydrated in an ethanol gradient, and treated in 10 mM Na-citrate buffer (pH 6.0) at 120°C for 10 min in a pressure cooker. The sections were incubated in a blocking buffer (1% BSA and 0.01% Tween 20 in 1× Tris-buffered PBS). Specifications of primary and secondary antibodies are described in Supplemental Experimental Procedures.

Cell and Crypt Scoring

Cells showing immune reactivity for eYFP and KLF4 and positive for EdU label were counted and scored within the crypts of the small intestine. The numbers were represented as the average of the total number of positive cells per positive crypt or as the fold change compared with basal levels.

TUNEL Assay

Histological sections were de-paraffinized and treated in 10 mM Na-Citrate buffer (pH 6.0) at 120°C for 3 min and cooled to room temperature. TUNEL assay for apoptotic cells was performed using the In Situ Cell Death Detection Kit, TMR red (Roche) as per manufacturer's instructions. Immunostaining for eYFP was carried as mentioned above. Cells showing immune reactivity for eYFP and positive for TMR label were scored within the crypts of the small intestine. The numbers were represented as the average of the total number of apoptotic cells per eYFP crypt.

Statistical Analysis

A linear mixed model for repeated measurements was used to estimate mean values and make comparisons among groups. Each mouse was treated as a random effect. Log transformation was used to make model assumptions when needed. Statistical analysis was carried out using SAS 9.3 (SAS Institute). Bars in each bar plot were 95% confidence interval of estimated means. In addition, Student's t test was performed using GraphPad Prism version 5.0 for Windows (GraphPad).

SUPPLEMENTAL INFORMATION

Supplemental Information includes Supplemental Experimental Procedures and three figures and can be found with this article online at http://dx.doi.org/10.1016/j.stemcr.2016.04.014.

AUTHOR CONTRIBUTIONS

J.G.K., C.-K.K., and A.M.G. performed the experiments, analyzed the data, and wrote the manuscript. A.B.B. analyzed the data and wrote the manuscript. V.W.Y. designed the experiments, analyzed the data, and wrote the manuscript.

ACKNOWLEDGMENTS

This research was supported by grants from the NIH (CA084197 and DK052230) to V.W.Y. C.-K.K. was supported by a T32 Medical Scientist Training Program grant (GM008444). We thank Dr. Jie Yang and Ivan Crnosija for support with statistical analysis.

Received: September 15, 2015
Revised: April 26, 2016
Accepted: April 26, 2016
Published: May 26, 2016

REFERENCES

Anno, G.H., Baum, S.J., Withers, H.R., and Young, R.W. (1989). Symptomatology of acute radiation effects in humans after exposure to doses of 0.5-30 Gy. Health Phys. *56*, 821–838.

Barker, N. (2014). Adult intestinal stem cells: critical drivers of epithelial homeostasis and regeneration. Nat. Rev. Mol. Cell Biol. *15*, 19–33.

Barker, N., van Es, J.H., Kuipers, J., Kujala, P., van den Born, M., Cozijnsen, M., Haegebarth, A., Korving, J., Begthel, H., Peters, P.J., et al. (2007). Identification of stem cells in small intestine and colon by marker gene Lgr5. Nature *449*, 1003–1007.

Buczacki, S.J., Zecchini, H.I., Nicholson, A.M., Russell, R., Vermeulen, L., Kemp, R., and Winton, D.J. (2013). Intestinal label-retaining cells are secretory precursors expressing Lgr5. Nature *495*, 65–69.

Cheng, H., and Leblond, C.P. (1974). Origin, differentiation and renewal of the four main epithelial cell types in the mouse small intestine. V. Unitarian theory of the origin of the four epithelial cell types. Am. J. Anat. *141*, 537–561.

Davies, P.S., Dismuke, A.D., Powell, A.E., Carroll, K.H., and Wong, M.H. (2008). Wnt-reporter expression pattern in the mouse intestine during homeostasis. BMC Gastroenterol. *8*, 57–72.

Evans, P.M., and Liu, C. (2008). Roles of Krupel-like factor 4 in normal homeostasis, cancer and stem cells. Acta Biochim. Biophys. Sin. (Shanghai) *40*, 554–564.

Gerdes, J., Schwab, U., Lemke, H., and Stein, H. (1983). Production of a mouse monoclonal antibody reactive with a human nuclear antigen associated with cell proliferation. Int. J. Cancer *31*, 13–20.

Ghaleb, A.M., Nandan, M.O., Chanchevalap, S., Dalton, W.B., Hisamuddin, I.M., and Yang, V.W. (2005). Kruppel-like factors 4 and 5: the yin and yang regulators of cellular proliferation. Cell Res. *15*, 92–96.

Ghaleb, A.M., Katz, J.P., Kaestner, K.H., Du, J.X., and Yang, V.W. (2007a). Kruppel-like factor 4 exhibits antiapoptotic activity following gamma-radiation-induced DNA damage. Oncogene *26*, 2365–2373.

Ghaleb, A.M., McConnell, B.B., Nandan, M.O., Katz, J.P., Kaestner, K.H., and Yang, V.W. (2007b). Haploinsufficiency of Kruppel-like factor 4 promotes adenomatous polyposis coli dependent intestinal tumorigenesis. Cancer Res. *67*, 7147–7154.

Ghaleb, A.M., Aggarwal, G., Bialkowska, A.B., Nandan, M.O., and Yang, V.W. (2008). Notch inhibits expression of the Kruppel-like factor 4 tumor suppressor in the intestinal epithelium. Mol. Cancer Res. *6*, 1920–1927.

Ghaleb, A.M., McConnell, B.B., Kaestner, K.H., and Yang, V.W. (2011). Altered intestinal epithelial homeostasis in mice with intestine-specific deletion of the Kruppel-like factor 4 gene. Dev. Biol. *349*, 310–320.

Luis, N.M., Morey, L., Di Croce, L., and Benitah, S.A. (2012). Polycomb in stem cells: PRC1 branches out. Cell Stem Cell *11*, 16–21.

McConnell, B.B., Ghaleb, A.M., Nandan, M.O., and Yang, V.W. (2007). The diverse functions of Kruppel-like factors 4 and 5 in epithelial biology and pathobiology. Bioessays *29*, 549–557.

Montgomery, R.K., Carlone, D.L., Richmond, C.A., Farilla, L., Kranendonk, M.E., Henderson, D.E., Baffour-Awuah, N.Y., Ambruzs, D.M., Fogli, L.K., Algra, S., et al. (2011). Mouse telomerase reverse transcriptase (mTert) expression marks slowly cycling intestinal stem cells. Proc. Natl. Acad. Sci. USA *108*, 179–184.

Powell, A.E., Wang, Y., Li, Y., Poulin, E.J., Means, A.L., Washington, M.K., Higginbotham, J.N., Juchheim, A., Prasad, N., Levy, S.E., et al. (2012). The pan-ErbB negative regulator Lrig1 is an intestinal stem cell marker that functions as a tumor suppressor. Cell *149*, 146–158.

Roche, K.C., Gracz, A.D., Liu, X.F., Newton, V., Akiyama, H., and Magness, S.T. (2015). SOX9 maintains reserve stem cells and preserves radio-resistance in mouse small intestine. Gastroenterology *149*, 1553–1563.e10.

Rowland, B.D., and Peeper, D.S. (2006). KLF4, p21 and context-dependent opposing forces in cancer. Nat. Rev. Cancer *6*, 11–23.

Rowland, B.D., Bernards, R., and Peeper, D.S. (2005). The KLF4 tumour suppressor is a transcriptional repressor of p53 that acts as a context-dependent oncogene. Nat. Cell Biol. *7*, 1074–1082.

Sangiorgi, E., and Capecchi, M.R. (2008). Bmi1 is expressed in vivo in intestinal stem cells. Nat. Genet. *40*, 915–920.

Sangiorgi, E., and Capecchi, M.R. (2009). Bmi1 lineage tracing identifies a self-renewing pancreatic acinar cell subpopulation capable of maintaining pancreatic organ homeostasis. Proc. Natl. Acad. Sci. USA *106*, 7101–7106.

Sellak, H., Wu, S., and Lincoln, T.M. (2012). KLF4 and SOX9 transcription factors antagonize beta-catenin and inhibit TCF-activity in cancer cells. Biochim. Biophys. Acta *1823*, 1666–1675.

Shields, J.M., Christy, R.J., and Yang, V.W. (1996). Identification and characterization of a gene encoding a gut-enriched Kruppel-like factor expressed during growth arrest. J. Biol. Chem. *271*, 20009–20017.

Takeda, N., Jain, R., LeBoeuf, M.R., Wang, Q., Lu, M.M., and Epstein, J.A. (2011). Interconversion between intestinal stem cell populations in distinct niches. Science *334*, 1420–1424.

Talmasov, D., Xinjun, Z., Yu, B., Nandan, M.O., Bialkowska, A.B., Elkarim, E., Kuruvilla, J., Yang, V.W., and Ghaleb, A.M. (2014). Kruppel-like factor 4 is a radioprotective factor for the intestine following gamma-radiation-induced gut injury in mice. Am. J. Physiol. Gastrointest. Liver Physiol. *308*, G121–G138.

Yan, K.S., Chia, L.A., Li, X., Ootani, A., Su, J., Lee, J.Y., Su, N., Luo, Y., Heilshorn, S.C., Amieva, M.R., et al. (2012). The intestinal stem cell markers Bmi1 and Lgr5 identify two functionally distinct populations. Proc. Natl. Acad. Sci. USA *109*, 466–471.

Zhang, W., Chen, X., Kato, Y., Evans, P.M., Yuan, S., Yang, J., Rychahou, P.G., Yang, V.W., He, X., Evers, B.M., et al. (2006). Novel cross talk of Kruppel-like factor 4 and beta-catenin regulates normal intestinal homeostasis and tumor repression. Mol. Cell Biol. *26*, 2055–2064.